HHS Public Access

Author manuscript

J Invest Dermatol. Author manuscript; available in PMC 2020 September 01.

Published in final edited form as:

J Invest Dermatol. 2020 September ; 140(9): 1698–1705.e1. doi:10.1016/j.jid.2019.12.033.

REDD1 (regulated in development and DNA damage 1) prevents dermal adipocyte differentiation and is required for hair cycle-dependent dermal adipose expansion

Guillermo C. Rivera-Gonzalez[1,2], **Anna Klopot**[3], **Kaitlyn Sabin**[1], **Gleb Baida**[3], **Valerie Horsley**[1,*], **Irina Budunova**[3,*]

[1]Department of Molecular, Cellular and Developmental Biology and Department of Dermatology, Yale University, New Haven, CT 06520

[2]Current address: Department of Developmental Biology, Washington University School of Medicine in St. Louis, St. Louis, MO, 63110

[3]Department of Dermatology, Northwestern University, Chicago, IL 60611

Abstract

Dermal white adipose (dWAT) expansion is associated with important homeostatic and pathologic processes in skin. Even though mammalian target of Rapamycin (mTOR)/Akt signaling is important for adipogenesis, the role of regulated in development and DNA damage 1 (REDD1), a negative regulator of mTOR/Akt, is poorly understood. Loss of REDD1 in mice resulted in reduction of body mass, total fat, size of gonadal white adipose tissue (WAT) and interscapular brown adipose tissue (BAT). Interestingly, inguinal subcutaneous WAT and dWAT in *REDD1* knockouts (KOs) were expanded compared to wild type (WT) mice. Size and number of mature adipocytes in dWAT were also increased in adult *REDD1* KOs. This dWAT phenotype was established around postnatal (PN) day 18, and did not depend on the hair growth cycle. Surprisingly, adipocyte precursor cells (APCs) numbers were lower in *REDD1* KO skin. *In vitro* analysis revealed increased differentiation of skin-derived *REDD1* KO APCs as indicated by higher lipid accumulation and increased adipogenic marker expression. 3T3L1 cells overexpressing REDD1 had decreased sensitivity to differentiation. Overall, our findings indicate that REDD1 silencing induced expansion of dWAT through hypertrophy and hyperplasia. This not

[*]Correspondence to: Irina Budunova, Department of Dermatology, Northwestern University, Ward Building 9-132, 303 East Chicago Avenue, Chicago, IL 60611, Phone: 312-503-4679; Fax: 312-503-4325, i-budunova@northwestern.edu, Valerie Horsley, Department of Molecular, Cell and Developmental Biology, Yale University, 219 Prospect St., Box 208103, New Haven, CT 06520, USA. valerie.horsley@yale.edu.

Author contributions: Conceptualization: GCR, IB, and VH; Investigation: GCR, GB, AK and KS; Formal Analysis: GCR, AK; Writing: GCR, IB, AK, and VH; Funding Acquisition: IB and VH.

Conflict of Interest

The authors state no conflicts of interests.

Data Availability

No datasets were generated or analyzed during the current study

previously reported REDD1-dependent mechanism of adipogenesis could be used to preferentially target skin-associated adipose tissue for therapeutic purposes.

Keywords

REDD1; dermal adipose; adipocyte; differentiation

INTRODUCTION

In mammals, white adipose tissue forms at specific body sites called depots. The major WAT depots include visceral depot in the abdomen (vWAT), subcutaneous adipose (sWAT), and dermal adipose within the dermis of the skin (dWAT) (Gesta et al., 2007). The expansion of vWAT and sWAT are regulated by metabolic stimuli. However, the expansion of dWAT is also associated with different physiological and pathological processes in skin such as hair follicle growth, injury, and bacterial infection (Plikus et al., 2008; Festa et al., 2011; Schmidt and Horsley 2013; Marangoni et al., 2015; Zhang et al., 2015, 2016; Plikus et al., 2017). The expansion of dWAT tissue, like other depots, is tied to the generation of new mature adipocytes (adipogenesis) by tissue resident adipocyte precursor cells (Rodeheffer et al., 2008; Festa et al., 2011; Plikus et al., 2017). Thus, the study of adipogenesis in the skin is required to understand how dWAT contributes to skin biology.

In mice, immature adipocytes in the skin first appear around embryonic day 16 (e16) and lipid-filled adipocytes can be observed by e18.5 (Wojciechowicz et al., 2013). In mature skin, the physiological expansion of dWAT is also closely associated with hair follicle growth. When hair follicles enter into the growth phase (anagen), dWAT also expands, and then decreases during catagen and telogen stages (Festa et al., 2011; Zhang et al., 2016; Foster et al., 2018). The mechanism by which hair follicles and dWAT coordinate their expansion is not completely understood and involves a crosstalk between mature adipocytes and APCs with transit amplifying and stem cells in the hair follicle (Plikus et al., 2008; Festa et al., 2011; Zhang et al., 2016). It has been proposed that both adipocyte hypertrophy (increased adipocyte size) and hyperplasia (increased adipocyte numbers driven by pre-adipocyte proliferation and differentiation) underlie increase of dWAT thickness during growth phase of hair cycle (Festa et al., 2011) whereas its regression during catagen and telogen is mostly driven by lipolysis (Foster et al., 2018).

Skin adipocyte precursor cells express a combination of surface markers that include PDGFRA, SCA-1, CD29, CD34 and CD24 (Festa et al., 2011). Recent studies have shown that APCs in the skin can be stimulated to proliferate and differentiate by extrinsic signaling such as Sonic Hedgehog (SHH), BMP, and PDGF (Rivera-Gonzalez et al., 2016; Zhang et al., 2016). Akt/mTORC1 signaling also plays a crucial role in adipogenesis and adipocyte differentiation, and its aberrations have been revealed in the models of obesity (Kim et al., 2002; Carnevalli et al., 2010). The important negative regulator of mTOR/Akt signaling is REDD1 (regulated in development and DNA damage response 1) also called DDIT4 (DNA damage-induced transcript 4) (Shoshani et al., 2002; Dennis et al., 2014; Baida et al., 2015). There is emerging evidence that REDD1 plays a prominent role in energy homeostasis

acting as a negative regulator of energy expenditure in major metabolic tissues including fat (Britto et al., 2018). Indeed, REDD1 expression was strongly increased in animal models of obesity and in obese patients (Elam et al., 2009; Williamson et al., 2014). Remarkably, *REDD1* KO mice appeared to be resistant to the development of obesity on a high-fat diet (Williamson et al., 2014). It was also shown that REDD1 regulates lipolysis and lipogenesis in cultured human and mouse adipocytes (Schupp et al., 2013). In our previous work, we showed that REDD1 plays an important role in skin where it is causatively involved in the development of glucocorticoid-induced skin atrophy: mice lacking REDD1 displayed cutaneous hyperplasia, and all skin compartments including dWAT appeared to be partially resistant to atrophy induced by chronic treatment with glucocorticoids (Baida et al., 2015).

The important roles of Akt/mTOR and REDD1 in adipogenesis, lipid metabolism, and energy homeostasis prompted us to look closer at the fat depots in *REDD1* KO animals with a specific focus on dWAT and regulation of adipocyte differentiation by REDD1. Unexpectedly, *REDD1* KO mice appeared to be lighter than wild type (WT) mice in the same genetic background and had significantly reduced total fat mass. However, *REDD1* KO mice have increased dWAT and subcutaneous fat (sWAT) depots. We found that dWAT extension was established early during postnatal skin development, in part due to the increased generation of new mature adipocytes and an influence on adipocyte differentiation. This extension of dWAT established at the early stages of postnatal development persisted via whole life of *REDD1* KO animals and was independent on hair cycle.

RESULTS

REDD1 loss negatively regulates body weight and gonadal and interscapular adipose depots but induces expansion of the dermal adipose layer

Akt/mTOR pathway plays an important role in adipocyte differentiation, and one of its major inhibitors, REDD1, is known to control energy homeostasis and lipogenesis. Thus, we assessed the effect of *REDD1* knockout on the different adipose tissue depots. First, we measured body weight, body composition, and the size of different fat depots in adult, 8 week old male and female WT and *REDD1* KO mice. We found a 15–20% decrease in total weight in *REDD1* KO mice of both sexes (Figure 1a). This was a consistent observation for numerous *REDD1* KO animal generations. *REDD1* KO animals also had significantly decreased total amount of fat and increased total body lean mass compared to WT animals as measured by EchoMRI™ (Table 1). Analysis of the size of selected fat depots (measured by weight) revealed a significant decrease in fat accumulation in gonadal WAT depot and interscapular brown adipose depot in *REDD1* KO mice (Figure 1a). Interestingly, the depots associated with skin: inguinal subcutaneous WAT (sWAT) and dWAT were significantly increased in *REDD1* KO animals (8 week old and older) of both sexes (Figure 1a–b.)

Next, we focused on the understanding of the mechanism(s) underlying the differential regulation of dWAT in *REDD1* KO. Both adipocyte hypertrophy (increased adipocyte size) and hyperplasia (increased adipocyte numbers driven by pre-adipocyte proliferation and differentiation) drive physiological increases in dWAT thickness (Festa et al., 2011; Foster et al., 2018). Thus, to further quantify the effect of REDD1 loss on dWAT, we assessed the size and number of Perilipin1+ mature dermal adipocytes. As shown in Figure 1b, there was a

dramatic difference in the thickness of the dWAT in *REDD1* KO compared to WT skin during the quiescent stage of the hair cycle (telogen, 8 week old mice). Morphometric analysis of Perilipin1+ adipocytes revealed that both the size and number of mature adipocytes were increased in *REDD1* KO skin (Figure 1c–e), suggesting that REDD1 silencing induced extension of dWAT via both hypertrophy and hyperplasia.

Decreased influence of hair follicle cycle on dWAT expansion in *REDD1* KO mice

Since physiological expansion of dWAT is closely associated with hair follicle growth, we further assessed whether REDD1 impacted dWAT size in a hair follicle cycle-dependent manner. We examined skin harvested at different stages of hair development and hair cycle: postnatal days 1–5 (shortly after hair follicle organogenesis occurs (Supplemental Figure 1), PN12 and 18 (during middle-late stages of hair follicle development) (Figure 2a), as well as PN20 (first telogen), and PN33 (subsequent anagen) (Figure 2b). We analyzed the differences in dWAT thickness by staining the skin with Oil Red O, a dye used for staining of neutral triglycerides and lipids and visualization of adipocytes (Figure Supplemental Figure 1 and Figure 2a) or by the expression of mature adipocyte marker Perilipin 1 (Figure 2b). No difference was detected in either dWAT thickness or hair follicle stage in WT and *REDD1* KO mice from PN1–12 (Supplemental Figure 1 and Figure 2a). However, after PN18, dWAT in *REDD1* KO mice of both sexes remained significantly thicker than in WT isogenic animals (Figure 2a). This dWAT phenotype was persistent and lasted throughout the life of the animals. Interestingly, during transition from telogen to subsequent anagen cycle at PN20 and PN33, we observed a significant increase in dWAT area in WT controls (as expected due to the regulation of adipogenesis during hair growth in WT animals), but no significant change in *REDD1* KO mice (Figure 2b), even though the dWAT in *REDD1* KOs remained significantly enlarged compared to WT animals. These results indicate that REDD1 regulates dWAT and mature adipocyte size prior to the first telogen phase of the hair cycle.

APCS in *REDD1* KO mice are reduced and directed toward differentiation

Our prior results showed that during the hair cycle, new mature adipocytes are generated from APCs (Rivera-Gonzalez et al. 2016). We hypothesized that the increase in dWAT adipocyte number may reflect an increase in APCs in *REDD1* KO skin. To test this hypothesis, we evaluated if there were any changes in the number of APCs in *REDD1* KO mice using FACS analysis of two populations of APCs: $CD29^{+}/CD34^{+}/Sca1^{+}/CD24^{-}$ preadipocytes and $CD29^{+}/CD34^{+}/Sca1^{+}/CD24^{+}$ adipocyte stem cells (Rodeheffer et al., 2008; Festa et al., 2011; Driskell et al., 2013; Rivera-Gonzalez et al., 2016). Surprisingly, *REDD1* KO skin contained fewer preadipocytes and adipocyte stem cells compared to WT skin (Figure 3b–c). Thus, dWAT expansion in *REDD1* KO mice was not due to an increase in APC number.

The reduction in APC number could be due to an increased propensity of APCs toward mature adipocyte differentiation, which would also increase dWAT size in *REDD1* KO skin. To test this possibility, we assessed whether loss of REDD1 expression altered the response of adipocyte precursors to known differentiation cues. To this end, we isolated APCs from WT and *REDD1* KO mice by FACS, and induced adipogenic differentiation *in vitro* with

insulin treatment. After 6 days in culture, *REDD1* KO APCs showed increased signs of differentiation as indicated by the high accumulation of intracellular lipid (Figure 4a–b). To further assess whether this increased lipid accumulation reflected increased adipogenic differentiation, we performed gene expression analysis of adipogenic markers by qPCR. The expression of adipogenic markers: *Cebpa*, *Pparg2*, *Adipoq,* and *Perilipin1* was significantly higher in *REDD1* KO compared to WT APCs (Figure 4c–f). These data indicate that REDD1 is necessary to suppress adipocyte differentiation in dermal APCs.

REDD1 overexpression prevents adipogenic differentiatio

To determine if REDD1 is sufficient to suppress adipocyte differentiation, we overexpressed REDD1 in 3T3-L1 cells and analyzed cell morphology and expression of mRNA and protein for markers of adipocyte differentiation (Figure 5a). After 12 days of adipogenic differentiation induction, 3T3L1-REDD1 cells showed decreased lipid accumulation (Figure 5b) and reduced expression of differentiation markers (Figure 5c) compared to control 3T3L1 cells. We also noted that phosphorylation of mTOR, and its down-stream substrates: S6 kinase, S6 ribosomal protein, and 4E-BP1 was not significantly different in 3T3L1-REDD1 cells and 3T3L1 cells despite significant overexpression of REDD1 (Figure 5d). Interestingly, the level of REDD1 was very high in untreated NIH3T3 cells which are resistant to adipogenesis compared to 3T3L1 cells sensitive to adipogenesis (Figure 5e). Taken together, our data indicate that REDD1 is both necessary and sufficient to suppress adipocyte differentiation in a manner that is independent from activation of mTOR signaling.

DISCUSSION

Our results showed that lack of REDD1 expression induces dWAT expansion fueled by the increased number and size of mature adipocytes and their elevated differentiation potential. These results are consistent with previous observations that downregulation of REDD1 in fruit flies and mammalian cells results in increased cell size, while overexpression of REDD1 results in a decreased cell size (Reiling and Hafen, 2004; Sofer et al., 2005). We demonstrated that REDD1 overexpression was sufficient to inhibit induction of late adipocyte differentiation markers (*PPARγ2*, *Perilipin1* and *Cebpa*) and significantly reduced cell ability to form lipid droplets *in vitro*. Consistent with our work, Gharibi and colleagues showed that stable knockdown of REDD1 in mesenchymal stem cells results in their accelerated differentiation toward adipocytes (increased staining with Oil Red O, increased expression of adipogenic genes e.g. *Pparγ*2) while the overexpression of REDD1 in these cells leads to reduction in expression of *Pparγ2* and *Cebpa* and greatly impaired ability of cells to differentiate into adipocyte lineage (Gharibi et al., 2016). Further, the effect of REDD1 overexpression on the ability of cells to differentiate was also found in other cell types suggesting a more general phenomenon. For example, overexpression of REDD1 in keratinocytes prevented induction of differentiation marker involucrin following calcium stimulated cell differentiation (Ellisen et al., 2002)

Interestingly, Schupp et al. showed that even though REDD1 overexpression tends to inhibit lipogenesis, the expression of adipocyte markers was not affected by REDD1 overexpression (Schupp et al., 2013). This inconsistency between our work and that of Schupp et al.

probably reflects the differences in cell type (3T3L1 cells vs C3H10T1/2) and type of REDD1 overexpression (constitutive versus transient). Our results suggest that REDD1 may also influence lipid release or lipolysis that is associated with hair follicle regression. The exact mechanism by which REDD1 controls lipid dynamics in adipose tissue will be an interesting area of future investigation.

It is well established that REDD1 is a negative regulator of mTOR signaling (Brugarolas et al., 2004; Sofer et al., 2005). However, our data suggests that effect of REDD1 on adipogenic differentiation is possibly mTOR-independent, which is consistent with other findings regarding mTOR-independence of some REDD1 effects (Schupp et al., 2013). Further, work of Regazzetti et al. suggests a rather intricate interplay between REDD1, mTOR and insulin in 3T3L1-adipocytes: in their experiments REDD1 was induced by insulin, and in turn, affected mTOR and insulin signaling (Regazzetti et al., 2012). Further work is required to better understand how constitutive alteration of REDD1 protein levels may affect adipocytes at the different stages of differentiation.

In addition, REDD1 status may be very important for lipogenesis and adipocyte hypertrophy that are important mechanisms of dWAT extension during natural HF cycle (Foster et al., 2018). Indeed, REDD1 plays very important role in the regulation of fatty acid and lipids metabolism and catabolism (Baida et al., 2015), and strongly affects function of the glucocorticoid receptor, one of the major regulators of lipolysis (Baida et al., 2015). Interestingly, REDD1 KO animals appeared to be partially resistant to steroid-induced dWAT hypoplasia (Baida et al., 2015), and REDD1 inhibitors were able to protect different skin compartments including dermal adipose against atrophy induced by topical glucocorticoids (Agarwal et al., 2019).

The differential regulation between dWAT and other WAT depots could also be caused by changes in systemic factors. Extracellular signaling is known to regulate adipogenesis (Lee, 2011) and changes in these external signals caused by REDD1 loss could differentially impact WAT depots given WAT inter and intra heterogeneity (Kwok et al., 2019).

One of the interesting findings reported here is that in the absence of REDD1, dWAT expansion occurs with little input from the hair follicle cycle. It is known that differentiation of APCs can be induced by transit-amplifying cells in the hair follicle through sonic-hedgehog signaling (Zhang et al., 2016) and that APCs can secrete molecules (possibly PDGFA) that can stimulate hair follicle growth (Festa et al., 2011). It remains to be investigated whether loss of REDD1 in dermal APCs mimics pro-adipogenic signals coming from the hair follicle or whether *REDD1* KO APCs can stimulate the hair follicle to produce these signals without inducing follicle growth. In either case, the *REDD1* KO animals provide an important model for the future studies focused on the dWAT/hair follicle crosstalk.

Overall, our results provide evidence for a REDD1-dependent skin-specific mechanism that regulates adipose tissue, which could be a key to generate therapeutic approaches that target specifically dermal adipose tissue without affecting other WAT depots. Moreover, our recent findings that REDD1 acts as atrophogene in skin (Baida et al., 2015), and that REDD1

inhibitors may prevent steroid-induced skin atrophy including hypoplasia of dWAT (Agarwal et al., 2019) proved the feasibility of REDD1-targeting in skin.

MATERIALS AND METHODS

Animals

The REDD1 KO breeder mice in F1 C57BL/6×129S genetic background were kindly provided by Quark Pharmaceuticals Inc. (Newark, CA); wild type (WT) isogenic C57BL/6×129S breeder mice were obtained from Taconic (Germantown, NY). Both colonies were bred at Northwestern University vivarium. Age and sex of animals used in the study are indicated in Results and Figure legends. The animal weight, size of WAT depots, and skin morphology were assessed in animals of both sexes. For body mass composition and FACS analysis of APC we mostly used female mice. All animal experiments were performed according to protocols approved by Northwestern University Animal Care and Use Committee.

Measurements of Fat Depot Weight and Body Composition

The *REDD1* KO and WT mouse body composition (fat, lean, free water, and total water mass) was measured in animals of both sexes using EchoMRI™ system at Northwestern Comprehensive Metabolic Core. Different fat depots in *REDD1* KO and WT animals of both sexes were isolated as published (Mann et al., 2014), weighed, and calculated as % of body mass to account for differences in body weight between individual mice.

Immunohistochemistry, Immunofluorescence and Morphometric Analysis

Mouse skin was embedded in either paraffin (for H&E and perilipin1 staining) or OCT (for Oil Red O staining). H&E staining was performed according to standard protocol and Oil Red O staining was performed as published (Feldman and Dapson, 1974). Perilipin1 staining (a marker of mature adipocytes) was performed as previously described (Festa et al., 2011) with Perilipin1 antibody (goat; Abcam, Cambridge, MA ab61682, 1:1,000). We measured either tissue thickness or area. For measurement of tissue thickness we used ZeissAxio Vision software and measured the length of the adipose tissue stained with Oil Red O. Adipose tissue area was measured in the image analysis software Fiji by outlining the perimeter and measuring the area of visible adipose tissue identified by perilipin staining. To normalize the measurements, the total area was divided by the length of the skin. For both measurement types at least 3 biological samples with 10 fields of view in each sample (totally 30 fields of view/ genotype) were analyzed.

FACS and Flow Cytometry

FACS analysis of adipocyte precursor cells was performed as described previously (Rivera-Gonzalez et al., 2016). To identify APCs, the stromal vascular fraction (SVF) was stained in 3% BSA in HBSS with the antibodies summarized in Supplemental Table 1. For live/dead cell discrimination, cells were stained with Sytox Orange (1:100,000; Invitrogen, Carlsbad, CA, S11368). Samples were sorted or analyzed with a FACS Aria III with DiVA software. Analysis of flow cytometry data was performed using FlowJo software.

Cell culture and adipogenic differentiation

3T3 L1 (CL-173) and NIH 3T3 (CRL-1658) embryonic fibroblasts were obtained from ATCC (Manassas, VA) and cultured as per manufacturers' recommendations.

Generation of 3T3L1 cells overexpressing REDD1

3T3L1 cells overexpressing human REDD1 protein under CMV promoter were generated by stable infection with lentiviruses. REDD1-expressing lentiviral suspension was obtained from Northwestern SDRC DNA/RNA delivery Core. REDD1-expressing 3T3L1 cells were selected with 4 μg/ml puromycin. Parental 3T3L1 were used as control.

In vitro adipocyte differentiation

For this protocol we used either FACS-isolated primary APCs plated on carboxyl-coated 24-well plates (BD Biosciences, 354775) or 3T3L1 cells. Figure 5a illustrates the protocol. Briefly, both cell types were grown to confluence and then serum-starved for 48h. After starving, primary APCs were stimulated with insulin (Sigma I1882, 1 μ/ml). Parental 3T3L1 and 3T3L1- REDD1 cells were stimulated with cocktail consisting of dexamethasone (Sigma D-4902, 0.1 μg/ml), 3-isobutyl-1-methylxanthine (IBMX, Sigma I58791G, 300 μg/ml) and insulin (Sigma I1882, 1 μg/ml). After 48h, both primary APCs and 3T3L1 cells were kept on insulin media (1 μg/ml) changed every 48h until harvested for further analysis. Lipid staining of differentiated 3T3L1 and 3T3L1-REDD1 cells was performed using Oil Red O (Electron Microscopy Sciences, Hatfield, PA, 26503–02) and visualized using bright field microscopy.

RNA isolation and real-time PCR

Total RNA was isolated using Trizol (Invitrogen, 15596–026) and RNeasy mini kit (QIAGEN, Germantown, MD, 74104), following the manufacturer's instructions. cDNA was synthesized using Superscript III First-Strand Synthesis System (Invitrogen, 18080051) and Oligo dT per the manufacturer's instructions. Real-time PCR was performed using SYBR green I Master mix (Roche Diagnostics Corporation, Indianapolis, IN, 04887352001) on a LightCycler 480 (Roche). Primers for specific genes are listed in Supplemental Table 2. Results were normalized to β-actin expression as described previously (Festa et al., 2011).

Western Blotting

3T3L1 and 3T3L1-REDD1 cells were collected in Cytobuster buffer (Sigma, 71009–3) supplemented with protease inhibitors. Protein lysates were subjected to Western blotting according to standard protocol. The primary antibodies used for Western blotting are listed in Supplementary Table 1.

Supplementary Material

Refer to Web version on PubMed Central for supplementary material.

Acknowledgements

This work was supported by R01GM112945, R01AI125366 (to IB), and by R01AR060296 (to VH). We are thankful to NU SDRC DNA/RNA delivery core supported by SDRC grant (1P30AR057216) for technical support. Histology services were provided by the Northwestern University Histology and Phenotyping Laboratory which is supported by NCI P30-CA060553 awarded to the Robert H Lurie Comprehensive Cancer Center.

Abbreviations

APC	adipocyte precursor cells
BAT	brown adipose tissue
dWAT	dermal white adipose tissue
IBMX	3-isobutyl-1-methylxanthine
HF	hair follicle
KO	knockout
mTOR	mammalian target of Rapamycin
REDD1	regulated in development and DNA damage 1
SVF	stromal vascular fraction
WAT	white adipose tissue
WT	wild type

References

Agarwal S, Mirzoeva S, Redhead B, Dudley JT, Budunova I. PI3K inhibitors protect against glucocorticoid-induced skin atrophy. EBioMedicine 2019;41: 526–37. [PubMed: 30737086]

Baida G, Bhalla P, Kirsanov K, Lesovaya E., Yakubovskaya M, Yuen K et al. REDD1 functions at the crossroads between the therapeutic and adverse effects of topical glucocorticoids. EMBO Mol Med 2015;7: 42–58. [PubMed: 25504525]

Britto FA, Cortade F, Belloum Y, Blaquiere M., Gallot YS Docquier A, et al. Glucocorticoid-dependent REDD1 expression reduces muscle metabolism to enable adaptation under energetic stress. BMC Biol 2018;16: 65. [PubMed: 29895328]

Brugarolas J, Lei K, Hurley RL, Manning BD, Reiling JH, Hafen E, et al. Regulation of mTOR function in response to hypoxia by REDD1 and the TSC1/TSC2 tumor suppressor complex. Genes & Development 2004;18: 2893–904. [PubMed: 15545625]

Carnevalli LS, Masuda K, Frigerio F, Le Bacquer O, Um SH, Gandin V, et al. S6K1 Plays a Critical Role in Early Adipocyte Differentiation. Dev Cell 2010;18: 763–74. [PubMed: 20493810]

Dennis MD, Coleman CS, Berg A, Jefferson LS, Kimball SR. REDD1 enhances protein phosphatase 2A-mediated dephosphorylation of Akt to repress mTORC1 signaling. Sci Signal 2014;7: ra68–8. [PubMed: 25056877]

Driskell RR, Lichtenberger BM, Hoste E, Kretzschmar K, Simon BD, Charalambous M, et al. Distinct fibroblast lineages determine dermal architecture in skin development and repair. Nature 2013;504: 277–81. [PubMed: 24336287]

Elam MB, Cowan GS, Rooney RJ, Hiler ML, Yallaturu CR, Deng X, et al. Hepatic gene expression in morbidly obese women: implications for disease susceptibility. Obesity (Silver Spring) 2009;17: 1563–73. [PubMed: 19265796]

Ellisen LW, Ramsayer KD, Johannessen CM, Yang A, Beppu H, Minda K, et al. REDD1, a developmentally regulated transcriptional target of p63 and p53, links p63 to regulation of reactive oxygen species. Mol Cell 2002;10: 995–1005. [PubMed: 12453409]

Feldman AT, Dapson RW. Relative effectiveness of various solvents for oil red O. Med Lab Technol 1974;31: 335–41. [PubMed: 4143062]

Festa E, Fretz J, Berry R, Schmidt B, Rodeheffer M, Horowitz M, et al. Adipocyte lineage cells contribute to the skin stem cell niche to drive hair cycling. Cell 2011;146: 761–71. [PubMed: 21884937]

Foster AR, Nicu C, Schneider MR, Hinde E, Paus R. Dermal white adipose tissue undergoes major morphological changes during the spontaneous and induced murine hair follicle cycling: a reappraisal. Arch Dermatol Res 2018;310: 453–62. [PubMed: 29704126]

Gesta S, Tseng Y-H, Kahn CR. Developmental origin of fat: tracking obesity to its source. Cell 2007;131: 242–56. [PubMed: 17956727]

Gharibi B, Ghuman M, Hughes FJ. DDIT4 regulates mesenchymal stem cell fate by mediating between HIF1α and mTOR signalling. Sci Rep 2016;6: 36889. [PubMed: 27876894]

Kim D-H, Sarbassov DD, Ali SM, King JE, Latek RR, Erdjument-Bromage H, et al. mTOR interacts with raptor to form a nutrient-sensitive complex that signals to the cell growth machinery. Cell 2002;110: 163–75. [PubMed: 12150925]

Kwok KHM, Lam KSL, Xu A. Heterogeneity of white adipose tissue: molecular basis and clinical implications. Experimental & Molecular Medicine 2019;11:e215

Lee M-J Hormonal Regulation of Adipogenesis. John Wiley & Sons, Inc. 2011; Hoboken, NJ, USA.

Mann A, Thompson A, Robbins N, Blomkalns AL. Localization, identification, and excision of murine adipose depots. J Vis Exp 2014;e52174–4.

Marangoni RG, Korman BD, Wei J, Wood TA, Graham LV, Whitfield ML, et al. Myofibroblasts in murine cutaneous fibrosis originate from adiponectin-positive intradermal progenitors. Arthritis Rheumatol 2015;67: 1062–73. [PubMed: 25504959]

Plikus MV, Guerrero-Juarez CF, Ito M, Li YR, Dedhia PH, Zheng Y, et al. Regeneration of fat cells from myofibroblasts during wound healing. Science 2017;355: 748–52. [PubMed: 28059714]

Plikus MV, Mayer JA, la Cruz de D, Baker RE, Maini PK, Maxson R, et al. Cyclic dermal BMP signalling regulates stem cell activation during hair regeneration. Nature 2008;451: 340–4. [PubMed: 18202659]

Regazzetti C, Dumas K, Le Marchand-Brustel Y, Peraldi P, Tanti JF, Giorgetti- Peraldi S. Regulated in development and DNA damage responses −1 (REDD1) protein contributes to insulin signaling pathway in adipocytes. PLoS ONE 2012;7: e52154. [PubMed: 23272222]

Rivera-Gonzalez GC, Shook BA, Andrae J, Holtrup B, Bollag K, Betscholtz C, et al. Skin Adipocyte Stem Cell Self-Renewal Is Regulated by a PDGFA/AKT-Signaling Axis. Cell Stem Cell. 2016;4:72–74

Reiling JH, Hafen E. The hypoxia-induced paralogs Scylla and Charybdis inhibit growth by down-regulating S6K activity upstream of TSC in Drosophila. Genes Dev. 2004;18:2879–92. [PubMed: 15545626]

Rodeheffer MS, Birsoy K, Friedman JM. Identification of White Adipocyte Progenitor Cells In Vivo. Cell 2008;135: 240–9. [PubMed: 18835024]

Schmidt BA, Horsley V. Intradermal adipocytes mediate fibroblast recruitment during skin wound healing. Development 2013;140: 1517–27. [PubMed: 23482487]

Schupp M, Chen F, Briggs ER, Rao S, Pelzmann HJ, Pessentheiner AR, Bogner-Strauss JG, et al. Metabolite and transcriptome analysis during fasting suggest a role for the p53-Ddit4 axis in major metabolic tissues. BMC Genomics 2013;14: 758. [PubMed: 24191950]

Shoshani T, Faerman A, Mett I, Zelin E, Tenne T, Gorodin S, et al. Identification of a novel hypoxia-inducible factor 1-responsive gene, RTP801, involved in apoptosis. Mol Cell Biol 2002;22: 2283–93. [PubMed: 11884613]

Sofer A, Lei K, Johannessen CM, Ellisen LW. Regulation of mTOR and Cell Growth in Response to Energy Stress by REDD1. Mol Cell Biol 2005;25: 5834–45. [PubMed: 15988001]

Williamson DL, Li Z, Tuder RM, Feinstein E, Kimball SR, Dungan CM. Altered nutrient response of mTORC1 as a result of changes in REDD1 expression: effect of obesity vs. REDD1 deficiency. J Appl Physiol 2014;117: 246–56. [PubMed: 24876363]

Wojciechowicz K, Gledhill K, Ambler CA, Manning CB, Jahoda CA. Development of the mouse dermal adipose layer occurs independently of subcutaneous adipose tissue and is marked by restricted early expression of FABP4. PLoS One. 2013;8:e59811. [PubMed: 23555789]

Zhang B, Tsai P-C, Gonzalez-Celeiro M, Chung O, Boumard B, Perdigoto CN, et al. Hair follicles' transit-amplifying cells govern concurrent dermal adipocyte production through Sonic Hedgehog. Genes & Development 2016;30: 2325–38. [PubMed: 27807033]

Zhang L-J, Guerrero-Juarez CF, Hata T, Bapat SP, Ramos R, Plikus MV, et al. Innate immunity. Dermal adipocytes protect against invasive Staphylococcus aureus skin infection. Science 2015;347: 67–71. [PubMed: 25554785]

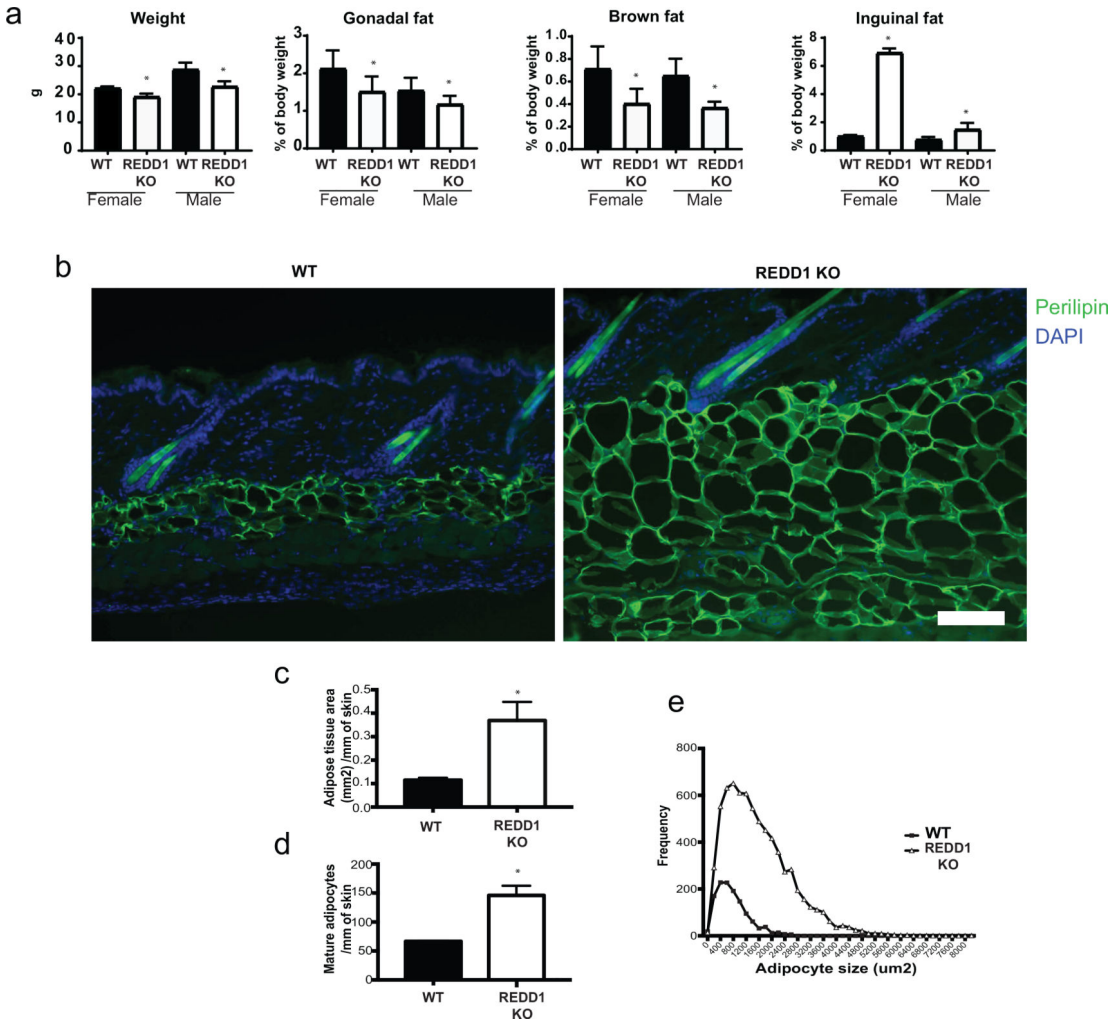

Figure 1. Differential effect of REDD1 loss on adipose depots: selective increase in dWAT and subcutaneous WAT.

a. Body weight and size of fat depots (% to total body weight) were measured in 8 week old WT and REDD1 KO animals, and presented as mean ±SD (N=5, for each sex/genotype). **b**. Representative images of Perilipin1+ mature adipocytes in dWAT layer in WT and REDD1 KO females. Scale bar=100μm. **c, d**. Quantification of dWAT area (c) and number of mature adipocytes (d) per mm of skin. **e**. Mature adipocyte size distribution in WT and REDD1 KO dWAT. At least 30 images of 3–5 individual skin samples from WT or REDD1 KO animals were analyzed. Data is presented as mean +/− SD. Statistically significant difference between REDD1 KO and WT: * $p<0.05$ (t-test for a, c, d).

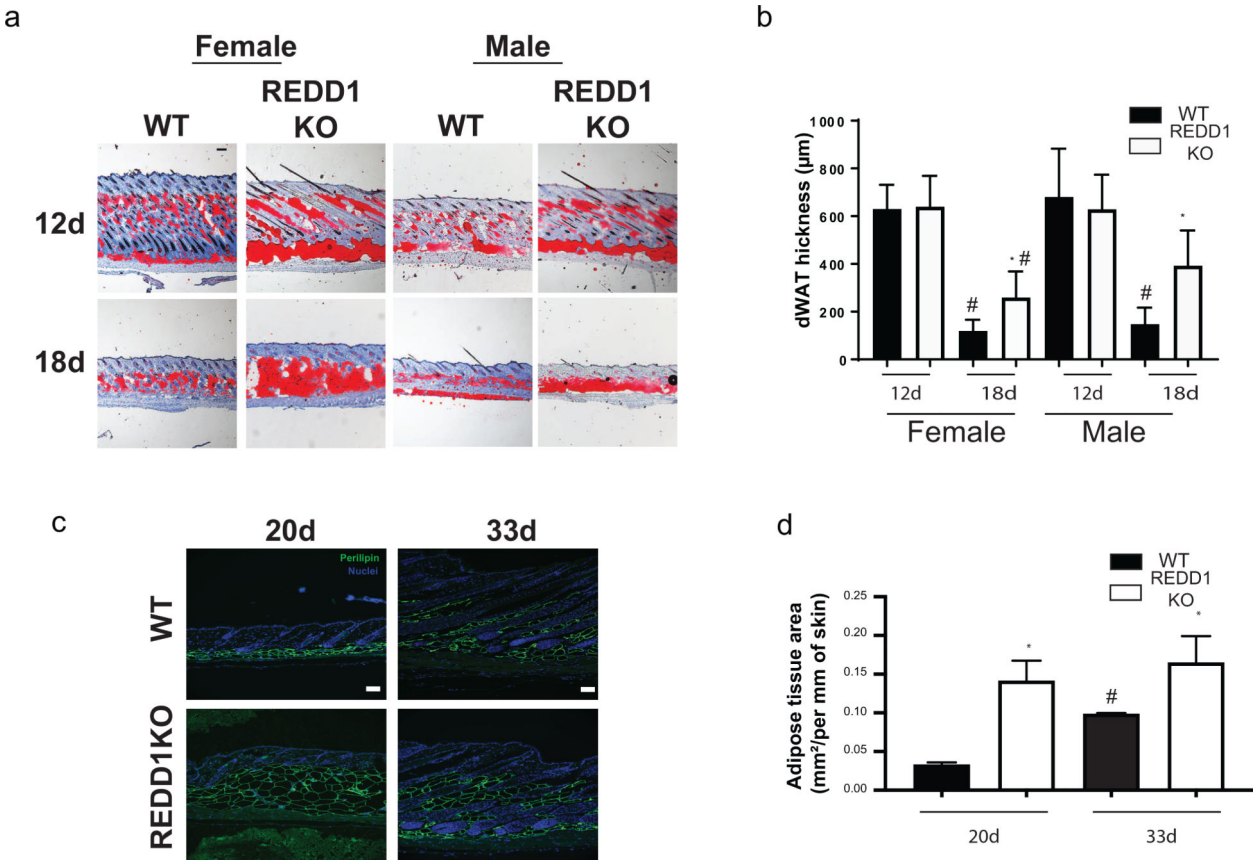

Figure 2. Differential regulation of dWAT during hair follicle cycling in WT and REDD1 KO animals.

a. Representative images of Oil Red O+ mature adipocytes in dWAT at PN 12 and 18. **b.** morphometric analysis of dWAT thickness (μm) at PN 12 and 18. **c**. Representative images of WT and *REDD1* KO female mouse skin at PN20 (Telogen) and PN33 (Anagen) stained for Perilipin1. **d**. Quantification of dWAT area/mm of skin during telogen and anagen stages. b, d Data are presented as average +/−SD. * indicates statistically significant differences between WT and REDD1 KO animals at $p<0.05$. # indicates statistically significant difference between animals of the same genotype but at different time points at $p<0.05$ (one-way ANOVA for b and d). Scale bars for (a, c) =100μm.

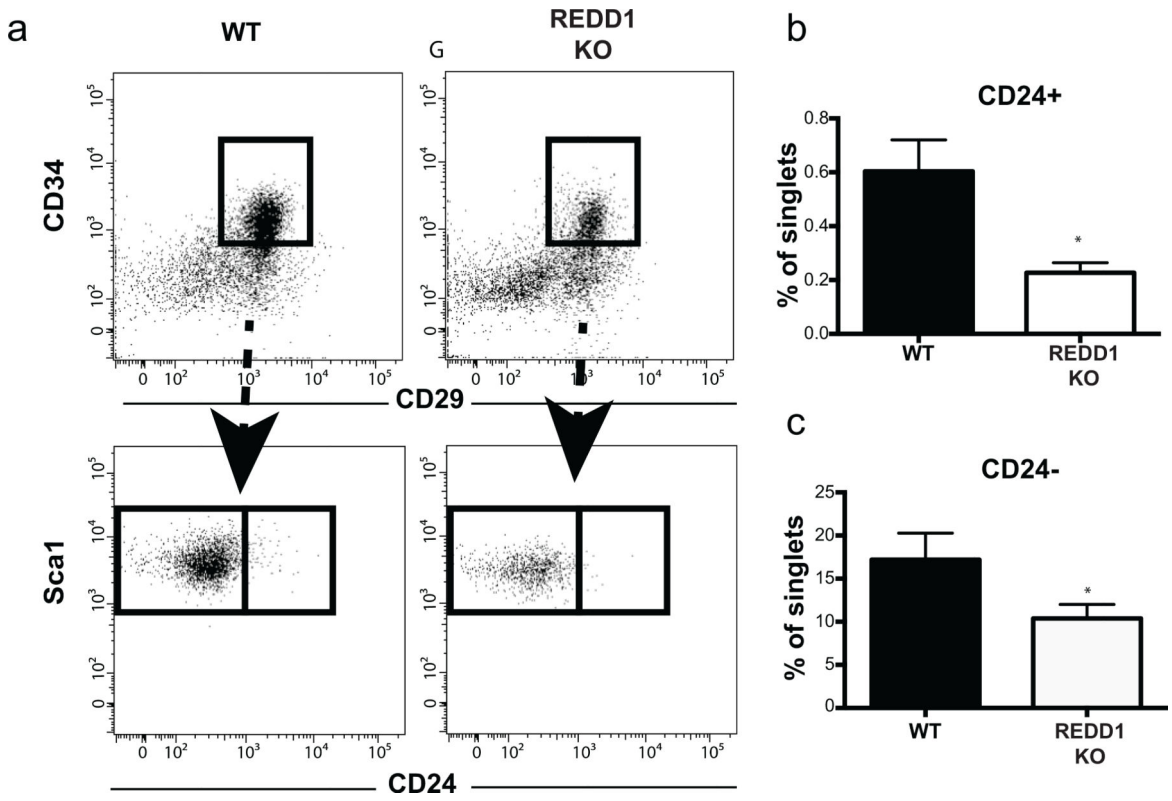

Figure 3. Decreased number of adipocyte precursors in REDD1 KO mouse skin.

a. Flow cytometry plots displaying the gating process to quantify the number of adipocyte stem cells (CD24+) and adipocyte precursors (CD24-) in 8 week old WT and REDD1 KO females. **b, c**. Number of adipocyte stem cell (CD24+) and preadipocytes (CD24-) is presented as % to all singlets. Data is presented as mean +/− SD for three different experiments. Statistically significant differences between WT and REDD1 KO animals * $p<0.05$ (t test).

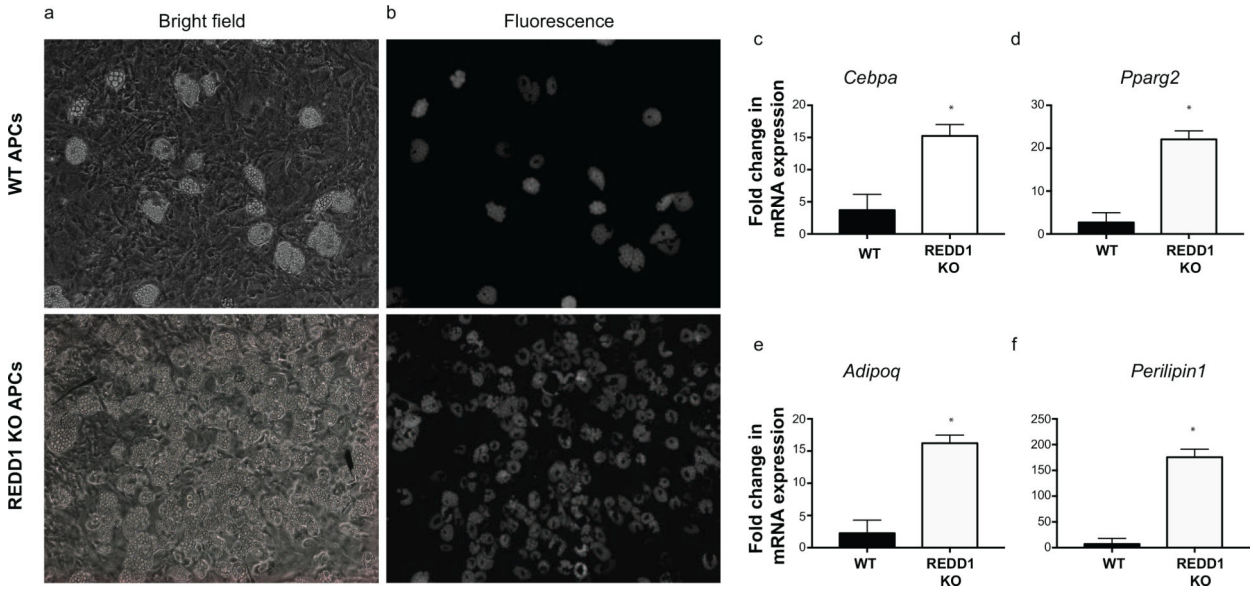

Figure 4. Loss of REDD1 expression promotes adipogenesis in vitro.

a-b. APCs were isolated from mouse skin by FACS (see Materials and Methods) using positive markers: CD29, CD34, and Sca1 and negative markers: CD31 and CD45. APCs were seeded in 24-well plates, 3×10^4 cells/well, and adipogenic differentiation was induced when cells reached confluence. Bright-field (a) and fluorescent (b) images of WT and REDD1 KO adipocyte precursors stained with Bodipy to visualize intracellular lipids at day 6 of adipogenic differentiation. **c-f**. RT-PCR expression of differentiation markers in adipocyte precursors at day 6 of adipogenic differentiation. Data is presented as mean +/− SD from three individual differentiation experiments. Statistically significant differences between WT and REDD1 KO adipocytes * $p<0.05$ (t test).

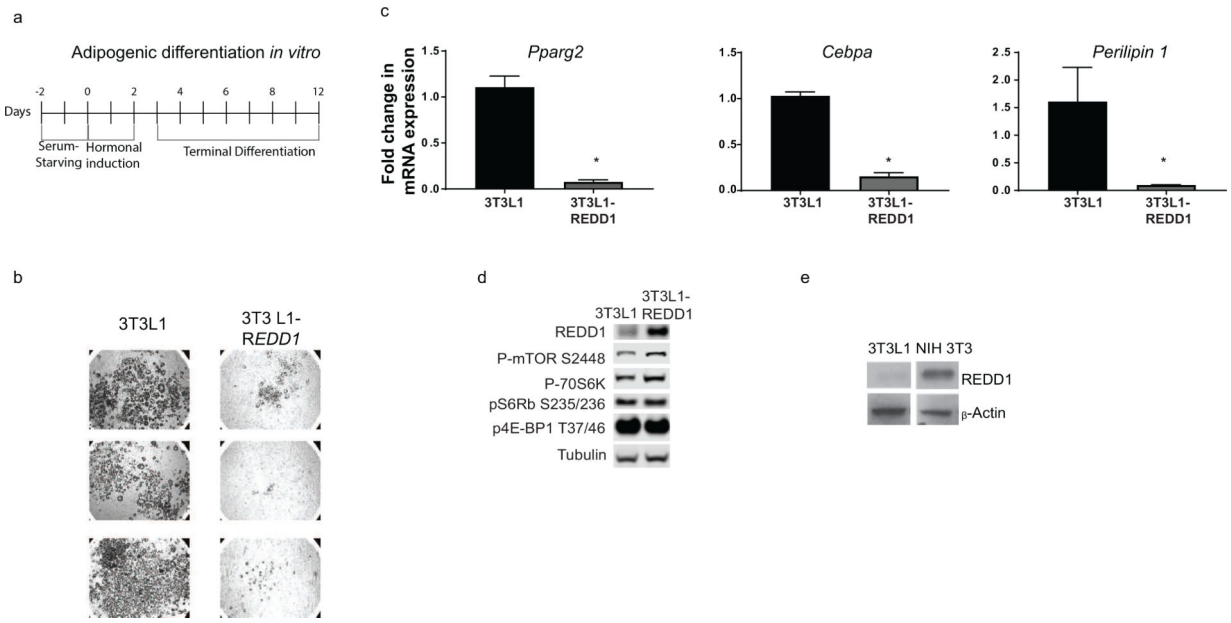

Figure 5. REDD1 controls early stages of adipogenic differentiation.

a. Timeline of adipogenic differentiation experiment. **b, c.** Adipogenic differentiation was induced in 3T3L1 (WT) and 3T3L1- REDD1 cells. Visualization of intracellular lipid accumulation (**b**, Oil Red O staining, three individual plates/cell type) and expression of differentiation markers (**c,** RT-PCR, three individual wells/cell type) 12 days after adipogenic induction. Statistically significant differences between WT and 3T3L1- REDD1 adipocytes: * $p<0.05$ (t test). **d.** Results of representative Western blot analysis of REDD1 expression and phosphorylation status of mTOR and its down-stream targets in 3T3L1 and 3T3L1- REDD1 cells. Tubulin was used as a loading control. **e.** Western Blot analysis of REDD1 expression in control 3T3L1 (adipogenic) and NIH3T3 (non-adipogenic) cells. β-Actin was used as loading control.

Table 1.

Decreased total fat mass in REDD1 KO animals.

Genotype	N	FAT (% BW)	Lean Mass (%BW)	Total Water (%BW)
WT	13	27.46±8.83	65.81±7.42	57.36±7.07
REDD1 KO	16	17.45±3.01***	75.14±2.96****	65.08±2.61***

Legend: Body mass composition was measured by EchoMRI in 8 week old isogenic WT and REDD1 KO 8 week old females (13–16 animals/genotype). Data are presented as mean +/− SD. Statistically significant difference between WT and REDD1 KOs

*** $p<0.001$ (two-tailed unpaired t- test).